POLITECNICO DI TORINO
Repository ISTITUZIONALE

High-power laser testing of calcium-phosphate-based bioresorbable optical fibers

Original
High-power laser testing of calcium-phosphate-based bioresorbable optical fibers / Peterka, Pavel; Pugliese, Diego; Jiíková, Bára; Boetti, Nadia G.; Turiová, Hana; Mirza, Inam; Borodkin, Andrei; Milanese, Daniel. - In: OPTICAL MATERIALS EXPRESS. - ISSN 2159-3930. - ELETTRONICO. - 11:7(2021), pp. 2049-2058. [10.1364/OME.428490]

Availability:
This version is available at: 11583/2905980 since: 2021-06-10T19:10:00Z

Publisher:
Optical Society of America

Published
DOI:10.1364/OME.428490

Terms of use:

This article is made available under terms and conditions as specified in the corresponding bibliographic description in the repository

Publisher copyright
Optica Publishing Group (formely OSA) postprint/Author's Accepted Manuscript

“© 2021 Optica Publishing Group. One print or electronic copy may be made for personal use only. Systematic reproduction and distribution, duplication of any material in this paper for a fee or for commercial purposes, or modifications of the content of this paper are prohibited.”

(Article begins on next page)

27 April 2024

Research Article | Vol. 11, No. 7 / 1 July 2021 / Optical Materials Express 2049

Optical Materials EXPRESS

High-power laser testing of calcium-phosphate-based bioresorbable optical fibers

PAVEL PETERKA,[1,*] DIEGO PUGLIESE,[2] BÁRA JIŘÍČKOVÁ,[1] NADIA G. BOETTI,[3] HANA TURČIČOVÁ,[4] INAM MIRZA,[4] ANDREI BORODKIN,[1] AND DANIEL MILANESE[5]

[1]*Institute of Photonics and Electronics (ÚFE) of the Czech Academy of Sciences (CAS), Chaberská 57, Prague, 182 51, Czech Republic*
[2]*Politecnico di Torino, Dipartimento di Scienza Applicata e Tecnologia (DISAT) and RU INSTM, Corso Duca degli Abruzzi 24, Torino, 10129, Italy*
[3]*Fondazione LINKS-Leading Innovation and Knowledge for Society, via P. C. Boggio 61, Torino, 10138, Italy*
[4]*HiLASE Ctr., Institute of Physics of the Czech Academy of Sciences (CAS), Za Radnici 828, Dolní Břežany, 252 41, Czech Republic*
[5]*Università di Parma, Dipartimento di Ingegneria e Architettura (DIA) and RU INSTM, Parco Area delle Scienze 181/A, Parma, 43124, Italy*
[*]*peterka@ufe.cz*

Abstract: Silica optical fibers are employed in endoscopy and related minimally invasive medical methods thanks to their good transparency and flexibility. Although silicon oxide is a biocompatible material, its use involves a serious health risk due to its fragility and the fact that potential fiber fragments can freely move inside the body without the possibility of being detected by conventional methods such as X-ray imaging. A possible solution to this issue can be the development of optical fibers based on bioresorbable (i.e., biodegradable and biocompatible) materials, which exhibit the important benefit of not having to be explanted after their functionality has expired. The optical power transmission tests of recently developed single-mode (SM) and multi-mode (MM) bioresorbable optical fibers based on calcium-phosphate glasses (CPGs) are here reported. A continuous-wave (CW) fiber laser at 1080 nm with output power up to 13 W and picosecond laser sources at 515 and 1030 nm with MW pulse peak power were used to test the transmission capabilities of the CPG fibers. No degradation of the CPG fibers transmission under long-term illumination by CW laser was observed. A laser-induced damage threshold (LIDT) at a fluence higher than 0.17 J/cm^2 was assessed with the picosecond laser sources.

© 2021 Optical Society of America under the terms of the OSA Open Access Publishing Agreement

1. Introduction

Optical fibers have been used in medicine for several decades, with applications in endoscopy, sensing and surgery, thanks to their unique properties such as small size, flexibility, transparency, non-toxicity and inertness to biological environment. Moreover, their immunity to electromagnetic field and radio frequency (RF) signals makes their use compatible with most diagnostic techniques, such as magnetic resonance imaging (MRI) and positron emission tomography (PET) as well as during thermal ablative treatments involving RF or microwave radiation [1–7]. Examples of low-invasive medical applications of high-power lasers include photodynamic and photo-thermal therapies [8–10], low-invasive surgery [3], kidney stone fragmentation [11,12], etc.

The availability of bioresorbable optical fibers can bring important benefits for the applications: potential fiber fragments that are unintentionally broken inside the body can dissolve in body fluids in a limited amount of time and do not need to be surgically extracted, as for conventional optical fibers. The dissolution rate can be tailored by the material composition as well as it

#428490 https://doi.org/10.1364/OME.428490
Journal © 2021 Received 29 Apr 2021; revised 30 May 2021; accepted 30 May 2021; published 10 Jun 2021

Optical Materials EXPRESS

depends on the environment. In particular, the rate of bioresorbability *in vivo* of the CPG fiber was found to be slower (0.3 μm/day) than that *in vitro* (1.4 μm/day) using regularly refreshed standard phosphate buffer saline (PBS) solution [13]. The possibility to implant these fibers in the body and leave them in place after their functionality has expired, without the need for retrieval, opens new perspectives in clinical applications. For example, they may be used to monitor in loco the healing process or detect inflammation after surgery or, in the brain, they could be employed to monitor deep hypoxia and hemorrhage in the sub-acute phase after brain injury [14,15]. Also, they could be used for interstitial photodynamic and photothermal therapies with in-situ laser irradiation [9,10].

Recently, inorganic CPG has been proposed as promising material to fabricate resorbable optical components, thanks to the possibility of tailoring its dissolution kinetics, as well as mechanical and optical properties, by conveniently changing the glass composition [7].

Bioresorbable optical fibers based on this glass were fabricated and showed enhanced optical properties, as they guarantee a wide window of transparency spanning from approximately 250 to 2600 nm and very low optical propagation loss of 1.9 and 4.7 dB/m, measured respectively at 1300 and 633 nm in SM CPG fiber. The bioresorbability and toxicity of the fibers were tested by means of *in vitro* dissolution tests [7] and *in vivo* experiments on male laboratory rats. The components of the CPG are not toxic and did not trigger any immune response in the *in vivo* tests [13].

In view of medical applications of bioresorbable CPG fibers that involve the use of high-power laser sources, both CW and pulsed, the investigation of their transmission capabilities in this power regime is of great interest. Phosphate glass material is known for its very high LIDT, comparable to that of fused silica [16,17], but higher attenuation and thermal issues limit phosphate glass fiber applications to much lower average powers, of the order of tens or hundred Watts [18,19]. So, although the phosphate glass-based optical fibers have been widely exploited for the development of laser sources and amplifiers [18,20,21], thanks to their excellent optical properties, high-power laser tests on the bioresorbable CPG optical fibers have not been performed yet.

This paper reports on the optical power transmission tests of recently developed SM and MM bioresorbable CPG optical fibers. A CW fiber laser operating at 1080 nm with output power up to 13 W was used to measure the long-term stability of the optical power transmitted through the CPG fibers. Other picosecond laser sources delivering 515 and 1030 nm wavelengths with MW pulse peak power were also used for the measurement of CPG fibers LIDT.

2. Materials and methods

The bioresorbable CPG optical fibers employed for the high-power laser tests were fabricated by preform drawing, with the preform being obtained by the rod-in-tube technique [6,7]. The core and cladding glasses were synthesized by melting a powder batch of high purity (99 +%) chemicals (P_2O_5, CaO, MgO, Na_2O, B_2O_3, SiO_2) inside an alumina crucible at a temperature of 1200 °C for 1 h, followed by casting into preheated brass molds. The core glass was cast into a cylindrical mold to form a 12 mm diameter rod, while the cladding glass tubes were shaped by rotational casting at a rotation speed of 3000 rpm using an equipment developed in-house. The SM and MM fibers, labeled as SMF and MMF, respectively, were obtained by drawing the respective core/cladding preform using a drawing tower developed in-house, whose furnace consists of a graphite ring heated by induction operating at 248 kHz and delivering 170 W to reach the drawing temperature (SAET, Torino, Italy). The refractive index profile of both the drawn CPG fibers was evaluated through the optical fiber analyzer IFA-100 [22,23]. Refractive index of the immersion oil was 1.5150 at 589.3 nm and 25 °C. The CPG fiber under test (F.U.T.) was spliced to the silica-based fiber using the fusion splicer Fitel S178A V2; small energy of the discharge and offsetting of the CPG fibers with respect to the discharge were employed so as to lower its heating [13]. The CPG fiber about 30 mm in length was pigtailed with the SM

Optical Materials EXPRESS

fiber Corning HI1060 and the MM fiber Thorlabs AFS105/125Y with 105 μm core, for the fiber-based laser source and free-space coupled laser testing, respectively. Note that the laser radiation was guided in the core in the case of fiber laser source, while it was guided in the whole fiber waveguide structure (with diameter 120 and 125 μm for the SM and MM fiber, respectively) in the case of the free-space coupled laser. Pigtailing of the phosphate fiber was necessary to mimic the actual practical usage of the phosphate fiber that is going to be used only at the end part of the probe, i.e., most of the fiber will be silica-based.

Lasers at wavelengths 515, 1030 and 1080 nm were used as they fall well into the low attenuation spectral range of the CPG fiber, e.g., CPG MM fiber displays minimum loss of 7 dB/m at 1300 nm and < 10 dB/m loss within 550-1600 nm [13]. Important low-invasive medical applications can be found in this spectral range including, e.g., endovenous laser ablation [24], sensing [13,15] and photodynamic therapy [9]. Lasers at 515 nm show high absorption in haemoglobin and have been used, e. g., for benign prostatic hyperplasia [8]. However, it should be noted that important medical lasers at wavelengths around 2 μm with high absorption in water [12] would be subject to losses > 40 dB/m at 2 μm in the CPG MM fiber [13]. An Ytterbium-doped fiber laser at the wavelength of 1080 nm was used for testing the CPG fiber transmission of the CW laser light and for long-term stability measurement, see an example of in-house developed Yb fiber ring laser in Fig. 1(a). The optical isolator ensured unidirectional operation of the laser and efficiently suppressed possible longitudinal-mode instabilities [25]. The isolator was located beyond the output coupler to prevent damage of the isolator. Since another isolator was placed at the output of the fiber laser, the CPG fiber could be cleaved perpendicularly without compromising the stability of the laser by back reflections [25–28]. The optical power was measured by the optical power detector Thorlabs S142C measuring up to 5 W (DET 1 in Fig. 1) and thermopile detector Gentech UP19K-110F-H5-D0 with incident power up to 100 W (DET 2 in Fig. 1).

The principal scheme for the measurement of the optical power transmission and LIDT of the CPG-based optical fibers using picosecond lasers with MW peak power is shown in Fig. 1(b). The first pulsed laser was the green beam at 515 nm produced as a frequency doubled fundamental laser beam operating at 1030 nm of the PERLA C100 laser system [29]. The pulse duration and repetition rate were 1.7 ps and 92 kHz, respectively. A critical phase-matched lithium triborate (LBO) crystal of 8 mm × 8 mm size and 10 mm length ($\theta = 90°$, $\varphi = 12.8°$, XY plane, anti-reflection (AR) coatings for 515 and 1030 nm) kept at a temperature of 47 °C was used for the frequency doubling. A half-wave plate and a polarizer were used for energy tuning. The beam diameter, expressed as a second moment beam width D4σ, was 2.6 mm at the crystal entrance. The generated second harmonic beam then reflected from two dichroic mirrors for the wavelength separation and after the second energy tuning system it was coupled into a MM 105/125 μm silica fiber via a positive lens of 150 mm focus. The spot focus size was thus around 40 μm. The MM fiber was spliced to the CPG fiber indicated in the scheme of Fig. 1(b) as F.U.T. The MM silica-based fiber helps to maintain the same illumination conditions for all samples as well as it is important to simulate potential applications where the CPG fibers are intended only for the final part of the optical fiber device. The tuning input power ranged from 100 mW up to 2 W (of 40 W available) providing focus spot fluence from 0.1 up to 2 J/cm^2.

The second pulsed laser system for LIDT measurement was a Pharos laser system (from Light Conversion) at 1030 nm, see Fig. 1(b). The pulse duration is tunable from 250 fs to 10 ps, with maximum average power of 6 W and corresponding pulse energy of 1 mJ. The repetition rate ranges between 1 and 200 kHz. For the experiment, a pulse duration of 6 ps and two repetition rates of 2 and 200 kHz were set. A half-wave plate and a polarizer were used for energy tuning. The beam was then coupled into the above-mentioned MM 105/125 μm silica fiber previously spliced to the CPG fiber via a positive lens of 150 mm focus. The tuning input average power was allowed to vary from 10 mW up to 1 W. The laser pulse duration at the output of CPG fiber

Optical Materials EXPRESS

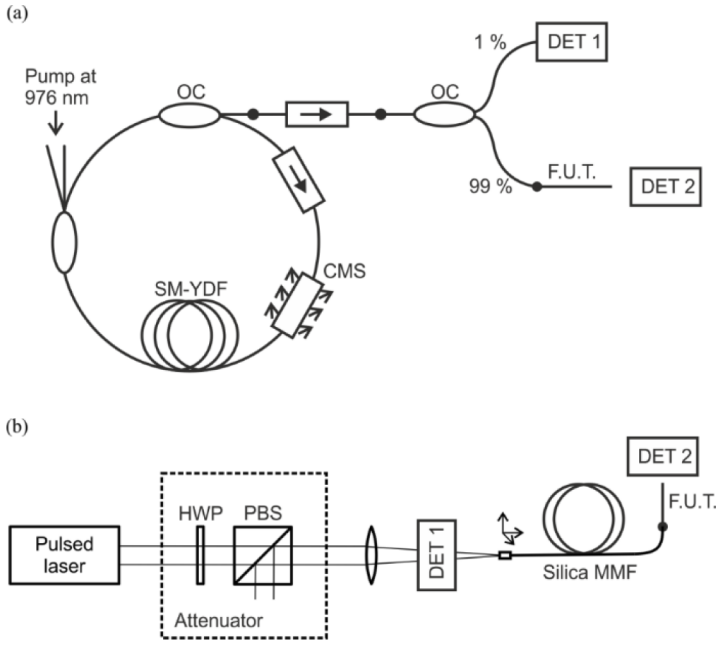

Fig. 1. Experimental set-ups employed for the measurement of the optical power transmission of the CPG fibers. The following three excitation sources were used: (a) CW Ytterbium fiber ring laser at 1080 nm, and (b) short-pulse laser beam at 515 nm or at 1030 nm. Legend: SM-YDF, single-mode Yb-doped fiber; OC, output coupler; CMS, cladding-mode stripper; DET, detector; HWP, half-wavelength plate; PBS, polarization beam splitter; MMF, multi-mode fiber; F.U.T, fiber under test.

samples was measured with the help of the Hamamatsu C10910 streak camera attached to an imaging spectrograph (Princeton instruments, SP2300), with a temporal resolution of ~ 15 ps. The main parameters of all the three lasers used in the tests are summarized in Table 1.

Table 1. Main parameters of the test lasers

Laser system / Provider	Operation regime	λ [nm]	Max. average power applied [W]	Pulse width [ps]	Rep. frequency [kHz]
FL22 / ÚFE CAS	CW	1080	13	-	-
PERLA C100 / HiLASE	pulsed	515	2	1.7	92
Pharos / Light Conversion	pulsed	1030	1	6	200 and 2

3. Results and discussion

Two CPG optical fibers, able to satisfy SM and MM behavior, respectively, were successfully fabricated by preform drawing and subsequently tested. Figure 2(a) depicts the typical neck-down region of the CPG fiber preform after the drawing process, while microscope photographs of the SMF and MMF samples end-face are shown in Fig. 2(b) and (c) and their refractive index profiles are reported in Fig. 2(d)-(f). The SMF showed diameters of 15 and 120 μm for the core and the cladding, respectively, while the corresponding values for the MMF are 45 and 125 μm.

The CPG fiber transmission of CW laser light was tested by the Yb-doped fiber ring laser with optical power up to 13 W at 1080 nm using the experimental set-up sketched in Fig. 1(a). Linear dependence of the CPG fiber output to the input power and no roll-off were observed,

Optical Materials EXPRESS

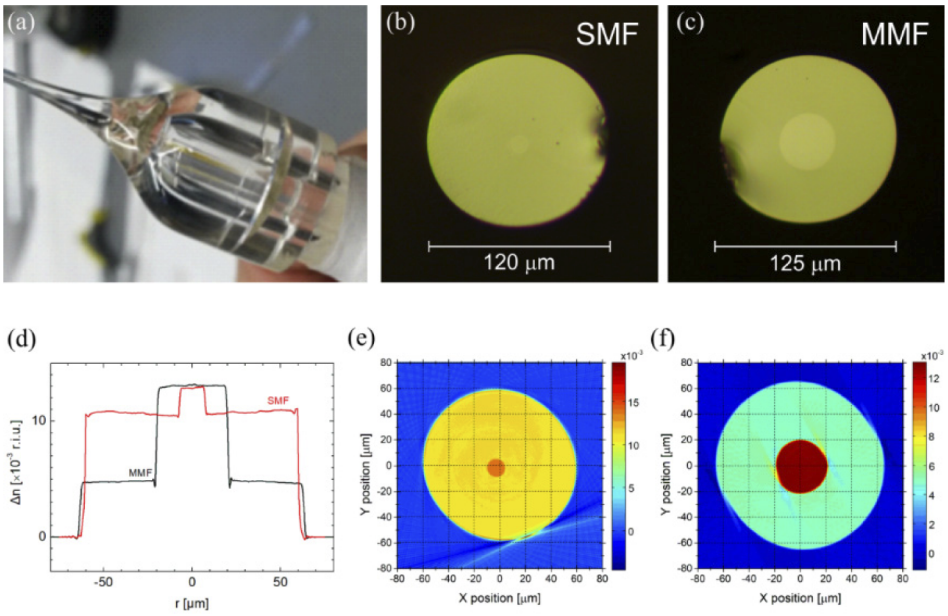

Fig. 2. (a) Neck-down zone of the CPG fiber preform after the drawing process, (b, c) optical microscope photographs of the bioresorbable CPG SM and MM fibers, (d) refractive index profile of the CPG fibers under test, (e, f) tomographic reconstruction of the refractive index profiles.

see Fig. 3(a). Long-term tests were performed by the same laser at the output for the SM and MM CPG fibers, see Fig. 3(b). A maximum heat load of 0.1 W/cm was estimated given the MM CPG fiber attenuation of 8 dB/m at 1080 nm. Such heat load can be cooled by airflow and it does not contribute to transmission change. Short-time relative variations of about ± 0.1% were observed for the SM and MM CPG fibers. Indeed, long-term fluctuations of the optical power sensor readings of ± 0.5% were found when the measurement uncertainty of the detectors was tested with a stable laser source. It should be noted that, while the laser monitor (1% branch of the optical fiber splitter) was firmly connected to the S142C detector by using an FC/APC connector, the CPG fiber output was directed to the detector in free-space. Therefore, sudden change in the ambient environment may slightly affect the measurement.

The tests with the pulsed lasers were performed using the experimental set-up depicted in Fig. 2(b). Firstly, the PERLA C100 laser system at 515 nm was used. The tests started with the evaluation of the LIDT of all-silica-fiber pigtail using about 20 μm spot size made by expanding the beam two times in diameter by a variable beam expander. A non-linear regression was achieved at a fluence equal to 1.5 J/cm^2 (at average power of 380 mW and peak power of 2.4 MW of the PERLA C100 laser system), which is an indication of the LIDT value of the silica fiber. This value is comparable with other reports of LIDT for bulk silica material and silica-based optical fibers under ps-pulsed laser light illumination at 1064 nm, where a damage threshold fluence of ~3 J/cm^2 and a self-focusing limit of 1-4.5 MW were reported [30,31].

The damaged 105/125 μm fiber input end-face for two successive tests with a ~20 μm spot size beam is shown in Fig. 4(a). No damage, instead, was observed for a spot focus size increased to 40 μm by a telescope within the applied laser power levels, see Fig. 4(b). In addition, the input fiber end-face was placed slightly out of focus so that the spot size was even larger on the fiber end-face. The defocusing was done at the expense of lower coupling efficiency, which is estimated to be > 80%. Only after such experimental checking of the silica fiber damage had

Optical Materials EXPRESS

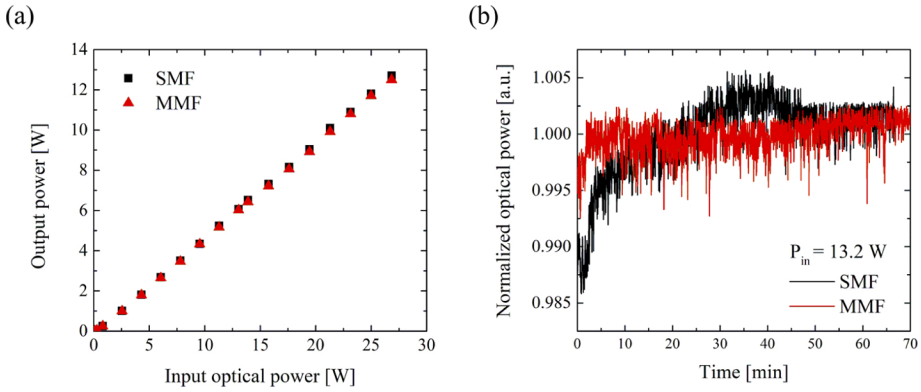

Fig. 3. Transmitted optical power (a) and stability of the optical power (b) through the SM and MM CPG optical fibers for the CW Ytterbium-doped fiber ring laser at 1080 nm. Note that the measured time variations are within the stability limits of the used optical power meters.

been completed, the tests continued with the evaluation of the LIDT of the bioresorbable CPG optical fibers.

The measurement of pulsed laser transmission of the MM CPG fiber at the PERLA C100 laser system is shown in Fig. 4(c). The slope of the linear part of the curve is 76%, while the attenuation of the 2 cm-long CPG fiber at 515 nm is about 7% (17 dB/m) [13]. Two distinct damage points denoted as A and B can be observed, see Fig. 4(c): while point A designates the transmission curve roll-off, point B represents the breakdown of the fiber. The damage can be

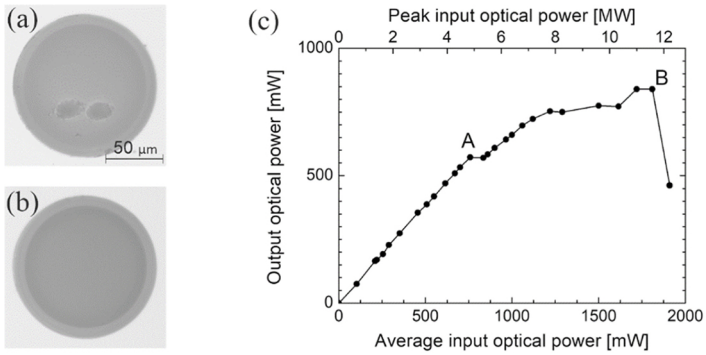

Fig. 4. Optical microscope photographs of the input fiber connector with 105/125 μm MM fiber: (a) connector damage when using ~20 μm spot size of the test beam, (b) the connector after tests with ~40 μm spot size of the test beam. (c) Optical power transmitted through the MM optical fiber spliced to MM CPG fiber for the pulsed laser system at 532 nm. The beginning of damage of the fiber is marked as A, while the detrimental break is marked as B. A line connecting the points is plotted just as an eye-guide.

attributed to the Kerr-lens self-focusing effect in the material of the CPG fiber at a free-space input peak power level of about 4 MW. It is worthwhile noting that due to dispersion of the 1 m-long MM fiber pigtail, the pulse width was broadened and the peak power inside the CPG fiber was lower than the input peak power. It shall be concluded that the self-focusing damage threshold of the CPG fiber is several times lower than that exhibited by bulk silica material under

Optical Materials EXPRESS

pulsed laser light illumination at 1064 nm, where self-focusing damage was reported at a peak power of 4.5 MW for a similar beam diameter [30,31].

The measurement of pulsed laser transmission of the MM CPG fiber at the second pulsed laser system (Pharos) with repetition rates of 200 and 2 kHz is shown in Figs. 5(a) and (b), respectively. Six identically prepared fiber samples were tested. More specifically, about 3 cm-long MM CPG sample was spliced to 0.3 m-long silica MM fiber with 105 µm core and FC/PC connector at the input. Because of the dispersion of the MM fiber pigtail, the pulse width was checked by the streak camera. The pulse width at the beginning of the CPG fiber was around 15 ps, which is given by the temporal resolution of the streak camera. Therefore, the input peak power in Fig. 5 shall be considered as a lower limit of the incident pulse peak power at the splice joint between the silica and the CPG fibers. No damage was observed for the 200 kHz regime of operation of the Pharos laser system where the input peak power was lower than 0.3 MW. Linear fits of the transmission measurement of samples #3 and #5 illuminated by 200 kHz train of pulses are shown in Fig. 5(a). For the repetition rate of 2 kHz, the damage was observed at peak powers higher than 1 MW, i.e., at a fluence higher than 0.17 J/cm^2, see Fig. 5(b). The fluence was estimated using a pulse width of 15 ps and illuminating the CPG fiber through the whole core area of the 105/125 µm MMF pigtail. No excessive heating of the fiber was observed and long-term tests were not performed.

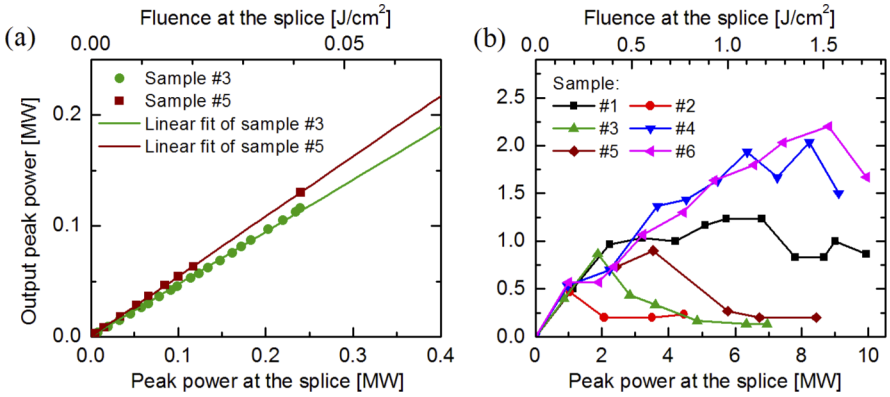

Fig. 5. Optical power transmitted through several samples of the MM CPG fiber in pulsed regime with repetition rates of 200 (a) and 2 kHz (b).

Optical microscope pictures of the CPG fiber samples after the pulsed laser tests are shown in Fig. 6. Note that the input connectors were also damaged for higher input peak power as shown in Fig. 6(a). Despite careful alignment of the FC/PC connector of the fiber samples with respect to the input beam by maximizing transmission at low powers, the input beam might not be always directed onto the fiber center, see damage of the sample #3 in Fig. 6(a). Such an offset damage of the fiber connector can be caused also by non-ideal pointing stability of the laser beam. The damage of the CPG fiber usually started close to the splice joint between the silica and the calcium-phosphate fibers, see Fig. 6(b) and 6(c). On the other hand, the free ends of the CPG fibers show no apparent damage, see Fig. 6(d)–6(f). It should be noted that the aim of this work was to test the LIDT of the as-prepared fibers, i.e., the fibers under test were not exposed to physiological fluids like it was during the *in vitro* and *in vivo* tests previously reported [7,13]. Exposure to such environment would surely determine possible applications of the bioresorbable CPG optical fibers. While core/cladding fiber waveguides with endcaps like the probes for pH-sensors [13] may work long time before being affected by bioresorption, other applications, namely with bare optical interface of the fiber and high-power transmission, will be limited to short-term applications. Additional tests in the future will include measuring the

Optical Materials EXPRESS

optical fiber transmission during dissolution tests in PBS solution or other similar physiological fluids.

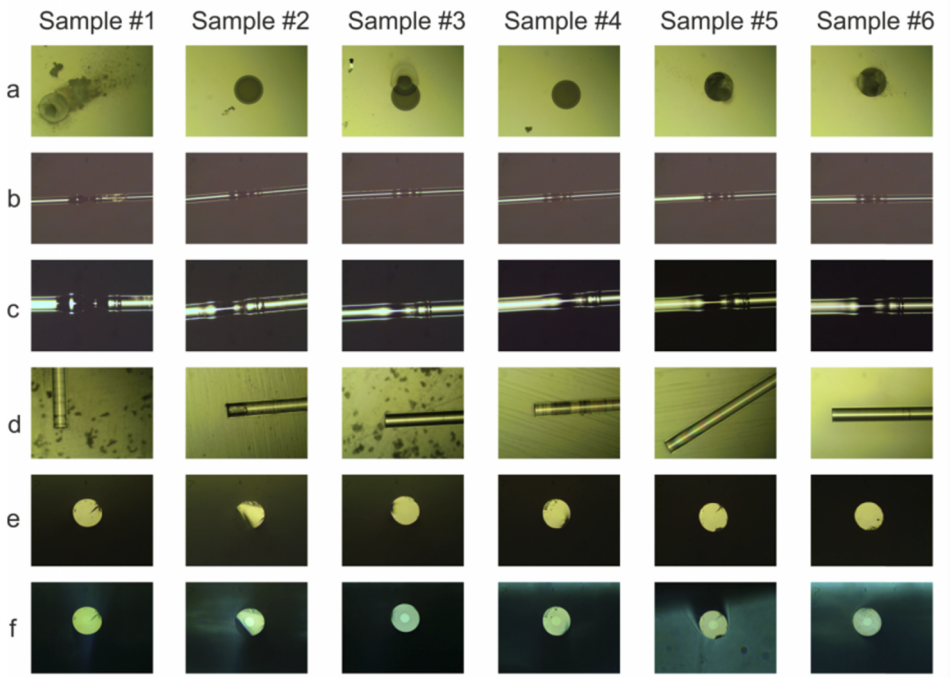

Fig. 6. Optical microscope photographs of different fiber samples after the pulsed laser tests: a - input fiber connector with 105/125 μm MM fiber; b, c - splice joint between the CPG and the MM silica fibers; d, e, f - end of the CPG fiber.

4. Conclusions

In this paper, high-power laser tests of bioresorbable optical fibers based on calcium-phosphate glass material have been reported for the first time to the authors' knowledge. The optical fibers withstood without changes long-term exposition to CW fiber lasers at around 1 μm and 13 W of incident optical power. In the case of ultrashort pulse regime, the LIDT values were found to be higher than 0.17 J/cm^2, i.e., only several times lower than the respective values in silica fibers. The presented results indicate that the developed bioresorbable fibers are suitable for high-power laser operation, both in CW and pulsed regime, paving the way towards the employment of these fibers for high-power laser therapeutic applications, especially those which can benefit from the possibility to leave the fiber in place after its function is completed, without the need to follow-up explant surgery.

Funding. Horizon 2020 Framework Programme (739573); Ministerstvo Školství, Mládeže a Tělovýchovy (CZ.02.1.01/0.0/0.0/15_003/0000445, CZ.02.1.01/0.0/0.0/15_006/0000674, LM2015086, LO1602); Grantová Agentura České Republiky (19-03141S).

Acknowledgements. This work was financially supported by the Strategy AV21 of the Czech Academy of Sciences, by the Interdepartmental Center PhotoNext of Politecnico di Torino and by the Czech Science Foundation under project No. 19-03141S. The authors from the HiLASE center of the Inst. of Physics of the CAS acknowledge support from the European Regional Development Fund, the state budget of the Czech Republic (project HiLASE CoE: Grant No. CZ.02.1.01/0.0/0.0/15_006/0000674), and by the European Union's Horizon 2020 research and innovation program under grant agreement No. 739573. This work was also supported by the Ministry of Education, Youth and Sports of the Czech Republic (Programs NPU I Project No. LO1602, and Large Research Infrastructure Project No. LM2015086 and project BIATRI, No. CZ.02.1.01/0.0/0.0/15_003/0000445). Portions of this work, i.e., preliminary

Optical Materials EXPRESS

results of MM fiber transmission using CW fiber laser and pulsed laser at 515 nm, were presented at the symposium SPIE Optics + Optoelectronics [32]. We greatly acknowledge help and support from our colleagues Pavel Honzátko, Jan Aubrecht, Ondřej Podrazký, Petr Vařák, Soňa Vytykáčová and Jana Proboštová from ÚFE CAS Prague, Davide Janner, Edoardo Ceci-Ginistrelli and Duccio Gallichi-Nottiani from Politechnico di Torino and Michael Písařík, Jiří Mužík, Ondřej Novák, Martin Smrž, Nadezhda Bulgakova and Tomáš Mocek from the HiLASE center.

Disclosures. The authors declare no conflicts of interest.

Data availability. Data underlying the results presented in this paper are not publicly available at this time but may be obtained from the authors upon reasonable request.

References

1. I. N. Papadopoulos, S. Farahi, C. Moser, and D. Psaltis, "High-resolution, lensless endoscope based on digital scanning through a multimode optical fiber," Biomed. Opt. Express **4**(2), 260–270 (2013).
2. J. I. Peterson and G. G. Vurek, "Fiber-optic sensors for biomedical applications," Science **224**(4645), 123–127 (1984).
3. M. Michalska, W. Brojek, Z. Rybak, P. Sznelewski, M. Mamajek, and J. Swiderski, "Highly stable, efficient Tm-doped fiber laser—a potential scalpel for low invasive surgery," Laser Phys. Lett. **13**(11), 115101 (2016).
4. S. A. Vasquez-Lopez, R. Turcotte, V. Koren, M. Plöschner, Z. Padamsey, M. J. Booth, T. Čižmár, and N. J. Emptage, "Subcellular spatial resolution achieved for deep-brain imaging in vivo using a minimally invasive multimode fiber," Light: Sci. Appl. **7**(1), 110 (2018).
5. O. Podrazký, J. Mrázek, J. Proboštová, I. Kašík, S. Pitrová, and K. Pavlíčková, "Monitoring of pH of the aqueous humour in cataract surgery using a fiber optic sensor," Fine Mech. Opt. **62**(11-12), 310–312 (2017).
6. D. Pugliese, M. Konstantaki, I. Konidakis, E. Ceci-Ginistrelli, N. G. Boetti, D. Milanese, and S. Pissadakis, "Bioresorbable optical fiber Bragg gratings," Opt. Lett. **43**(4), 671–674 (2018).
7. E. Ceci-Ginistrelli, D. Pugliese, N. G. Boetti, G. Novajra, A. Ambrosone, J. Lousteau, C. Vitale-Brovarone, S. Abrate, and D. Milanese, "Novel biocompatible and resorbable UV-transparent phosphate glass based optical fiber," Opt. Mater. Express **6**(6), 2040–2051 (2016).
8. Ł. Dołowy, W. Krajewski, J. Dembowski, R. Zdrojowy, and A. Kołodziej, "The role of lasers in modern urology," Cent. Eur. J. Urol. **68**(2), 175–182 (2015).
9. Z. Huang, "A review of progress in clinical photodynamic therapy," Technol. Cancer Res. Treat. **4**(3), 283–293 (2005).
10. P.-J. Lou, H. R. Jäger, L. Jones, T. Theodossy, S. G. Bown, and C. Hopper, "Interstitial photodynamic therapy as salvage treatment for recurrent head and neck cancer," Br. J. Cancer **91**(3), 441–446 (2004).
11. A. A. Boni, D. I. Rosen, S. J. Davis, and L. A. Popper, "High-power laser applications to medicine," J. Quant. Spectrosc. Radiat. Transfer **40**(3), 449–467 (1988).
12. P. Kronenberg and O. Traxer, "The laser of the future: reality and expectations about the new thulium fiber laser—a systematic review," Transl. Androl. Urol. **8**(S4), S398–S417 (2019).
13. O. Podrazký, P. Peterka, I. Kašík, S. Vytykáčová, J. Proboštová, J. Mrázek, M. Kuneš, V. Závalová, V. Radochová, O. Lyutakov, E. Ceci-Ginistrelli, D. Pugliese, N. G. Boetti, D. Janner, and D. Milanese, "In-vivo testing of a bioresorbable phosphate-based optical fiber," J. Biophotonics **12**(7), e201800397 (2019).
14. J. G. Kim and H. Liu, "Variation of haemoglobin extinction coefficients can cause errors in the determination of haemoglobin concentration measured by near-infrared spectroscopy," Phys. Med. Biol. **52**(20), 6295–6322 (2007).
15. S. Turtaev, I. T. Leite, T. Altwegg-Boussac, J. M. P. Pakan, N. L. Rochefort, and T. Čižmár, "High-fidelity multimode fibre-based endoscopy for deep brain in vivo imaging," Light: Sci. Appl. **7**(1), 92 (2018).
16. J. H. Campbell and T. I. Suratwala, "Nd-doped phosphate glasses for high-energy/high-peak-power lasers," J. Non-Cryst. Solids **263-264**, 318–341 (2000).
17. G. Shi, S. Fu, Q. Sheng, J. Li, Q. Fang, H. Liu, A. Chavez-Pirson, N. Peyghambarian, W. Shi, and J. Yao, "Megawatt-peak-power picosecond all-fiber-based laser in MOPA using highly Yb^{3+}-doped LMA phosphate fiber," Opt. Commun. **411**, 133–137 (2018).
18. Y.-W. Lee, M. J. F. Digonnet, S. Sinha, K. E. Urbanek, R. L. Byer, and S. Jiang, "High-power Yb^{3+}-doped phosphate fiber amplifier," IEEE J. Sel. Top. Quantum Electron. **15**(1), 93–102 (2009).
19. L. Kotov, M. Akbulut, A. Chavez-Pirson, J. Zong, and N. Peyghambarian, "More than 100W, 18 cm Yb-doped phosphate fiber amplifier," Proc. SPIE **10897**, 32 (2019).
20. A. Schülzgen, L. Li, X. Zhu, V. L. Temyanko, and N. Peyghambarian, "Microstructured active phosphate glass fibers for fiber lasers," J. Lightwave Technol. **27**(11), 1734–1740 (2009).
21. M. Franczyk, R. Stępień, B. Piechal, D. Pysz, K. Stawicki, B. Siwicki, and R. Buczyński, "High efficiency Yb^{3+}-doped phosphate single-mode fibre laser," Laser Phys. Lett. **14**(10), 105102 (2017).
22. A. D. Yablon, "Multi-wavelength optical fiber refractive index profiling by spatially resolved Fourier transform spectroscopy," J. Lightwave Technol. **28**(4), 360–364 (2010).
23. A. D. Yablon, "New transverse techniques for characterizing high-power optical fibers," Opt. Eng. **50**(11), 111603 (2011).
24. C. Karathanos, K. Spanos, K. Batzalexis, P. Nana, G. Kouvelos, N. Rousas, and A. D. Giannoukas, "Prospective comparative study of different endovenous thermal ablation systems for treatment of great saphenous vein reflux," J. Vasc. Surg. Venous Lymphat. Disord. **9**(3), 660–668 (2021).

Optical Materials EXPRESS

25. P. Peterka, P. Koška, and J. Čtyroký, "Reflectivity of superimposed Bragg gratings induced by longitudinal mode instabilities in fiber lasers," IEEE J. Sel. Top. Quantum Electron. **24**(3), 1–8 (2018).
26. P. Peterka, P. Navrátil, J. Maria, B. Dussardier, R. Slavík, P. Honzátko, and V. Kubeček, "Self-induced laser line sweeping in double-clad Yb-doped fiber-ring lasers," Laser Phys. Lett. **9**(6), 445–450 (2012).
27. P. Navratil, P. Peterka, P. Vojtisek, I. Kasik, J. Aubrecht, P. Honzatko, and V. Kubecek, "Self-swept erbium fiber laser around 1.56 μm," Opto-Electron. Rev. **26**(1), 29–34 (2018).
28. J. Aubrecht, P. Peterka, P. Koška, O. Podrazký, F. Todorov, P. Honzátko, and I. Kašík, "Self-swept holmium fiber laser near 2100 nm," Opt. Express **25**(4), 4120–4125 (2017).
29. M. Smrž, O. Novák, J. Mužík, H. Turčičová, M. Chyla, S. S. Nagisetty, M. Vyvlečka, L. Roškot, T. Miura, J. Černohorská, P. Sikocinski, L. Chen, J. Huynh, P. Severová, A. Pranovich, A. Endo, and T. Mocek, "Advances in high-power, ultrashort pulse DPSSL technologies at HiLASE," Appl. Sci. **7**(10), 1016 (2017).
30. A. V. Smith and B. T. Do, "Bulk and surface laser damage of silica by picosecond and nanosecond pulses at 1064 nm," Appl. Opt. **47**(26), 4812–4832 (2008).
31. A. V. Smith, B. T. Do, G. R. Hadley, and R. L. Farrow, "Optical damage limits to pulse energy from fibers," IEEE J. Sel. Top. Quantum Electron. **15**(1), 153–158 (2009).
32. P. Peterka, M. Písařík, H. Turčičová, J. Černohorská, O. Podrazký, P. Honzátko, P. Vařák, D. Pugliese, N. G. Boetti, D. Gallichi-Nottiani, D. Janner, and D. Milanese, "High-power laser tests of phosphate glass-based bioresorbable optical fibers transmission," Proc. SPIE **11029**, 40 (2019).

130.192.232.214 ns 2021-06-10 11:58:50